The DOI for this manuscript is doi: 10.1175/2009JCLI3139.1

Importance of Ocean Heat Uptake Efficacy to Transient Climate Change

Michael Winton
Geophysical Fluid Dynamics Laboratory/NOAA, Princeton, New Jersey

Ken Takahashi
AOS Program, Princeton University, Princeton, New Jersey

Isaac M. Held
Geophysical Fluid Dynamics Laboratory/NOAA and Princeton University, Princeton, New Jersey

Accepted for *Journal of Climate*

1 November 2009

Corresponding author address: Michael Winton, NOAA/GFDL, Princeton University Forrestal Campus, 201 Forrestal Rd., Princeton, NJ 08540.
E-mail: Michael.Winton@noaa.gov

Abstract

We propose a modification to the standard forcing/feedback diagnostic energy balance model to account for 1) differences between effective and equilibrium climate sensitivities and 2) the variation of effective sensitivity over time in climate change experiments with coupled atmosphere-ocean climate models. In the spirit of Hansen et al (2005) we introduce an efficacy factor to the ocean heat uptake. Comparing the time-evolution of the surface warming in high and low efficacy models demonstrates the role of this efficacy in the transient response to CO_2 forcing. Abrupt CO_2 increase experiments show that the large efficacy of the Geophysical Fluid Dynamics Laboratory's CM2.1 model sets up in the first two decades following the increase in forcing. The use of an efficacy is necessary to fit this model's global mean temperature evolution in periods with both increasing and stable forcing. The inter-model correlation of transient climate response with ocean heat uptake efficacy is greater than its correlation with equilibrium climate sensitivity in an ensemble of climate models used for the 3rd and 4th IPCC assessments. When computed at the time of doubling in the standard experiment with 1%/yr increase in CO_2, the efficacy is variable amongst the models but is generally greater than 1, averages between 1.3 and 1.4, and is as large as 1.75 in several models.

1. Introduction

The familiar linear zero-dimensional energy balance model is a useful tool for summarizing and analyzing the response of global mean surface temperature to radiative forcing in simulations of forced climate change. Once tuned to a target atmosphere-ocean general circulation model (AOGCM), the hope is that the simple model can be used to predict how the AOGCM would respond to a large range of forcings (e.g. IPCC 2007, Meinshausen et al 2008).

The equilibrium climate sensitivity of the linear energy balance model is one of the key parameters adjusted to mimic the target AOGCM. However, rather than the equilibrium sensitivity, which is usually estimated using an atmosphere/slab-ocean model, an "effective sensitivity" (Murphy, 1995) is often used for this exercise, determined from a transient run of the AOGCM (IPCC 2007, Table S8.1), in an attempt to avoid inconsistencies between AOGCM and slab ocean sensitivities. The effective sensitivity is obtained by scaling up the transient temperature response by the factor R/(R-N), where R is the radiative forcing and N is the top-of-atmosphere heat uptake (we refer to this informally as the ocean heat uptake in the following since the two are nearly the same on the timescales of interest here). The great majority of AOGCMs with available data in the IPCC third and fourth assessment reports (IPCC 2001; IPCC 2007) have effective sensitivities less than their equilibrium sensitivities. However, several researchers have noted an increase in the effective sensitivity over the course of long climate change simulations (Senior and Mitchell 2000; Gregory et al 2004), although this result is not

universal (Watterson 2000; Boer and Yu 2003). The increase in effective sensitivity is expected as a model with an effective sensitivity less than its equilibrium sensitivity approaches equilibrium.

Williams et al (2008) examined the relationship between the top-of-atmosphere (TOA) fluxes and the surface temperature change in the stabilized-CO_2 section of 1% CO_2 increase experiments and defined an "effective forcing" by extrapolating this relationship back to a zero temperature change. Six of the eight models they investigated had effective forcings that were less than the traditionally defined radiative forcings. They argue that this is evidence for a direct CO_2 effect on clouds, with fixed ocean temperatures, which modifies the "forcing" in analogy to the familiar direct stratospheric response. Gregory and Webb (2008) discuss an analogous analysis of slab ocean models; however, the time scale of forcing adjustment in Williams et al is on the order of decades, implicating oceanic adjustment as an important factor and favoring a feedback interpretation.

In this study, we propose an alternative interpretation of "effective forcing" and the time variation of "effective sensitivity". We are inspired by Hansen et al (2005), who noted that different forcing agents resulting in the same global mean radiative forcing can elicit different global mean temperature responses and accounted for this by introducing an efficacy factor associated with each forcing (see also IPCC 2007, section 2.8.5). In this paper we note that an efficacy can also be applied to ocean heat uptake. It might seem perverse to treat ocean heat uptake as a forcing rather than a feedback when it is clearly internal to the climate system and likely varies with global mean temperature change.

One way of rationalizing this approach is to consider a slab-ocean model in which one attempts to mimic the fully coupled system by specifying the heat flux exchanged between the deep ocean and the slab, putting aside the question of how the heat uptake is determined. A linear zero-dimensional model of this system would have as its inputs the heat uptake as well as the radiative forcing, leading one to consider the possibility of non-unitary efficacy of the heat uptake. We argue in the following that non-unitary efficacy of ocean heat uptake is a useful alternative to thinking in terms of effective forcings or the time-variation of effective sensitivity.

In section 2 we present a model comparison that motivates the need for an ocean heat uptake efficacy and demonstrate that the feedbacks that apply to ocean forcing can be significantly different than those that apply to CO_2 forcing. In section 3 we define non-dimensional quantities that allow us to compare efficacies when radiative forcing and equilibrium sensitivity vary in time and between models. In section 4 we look at the ability of ocean heat uptake efficacy to characterize the time evolution of the climate state in a particular model – the GFDL CM2.1. The distribution of efficacies in the IPCC multi-model ensembles of idealized transient climate change experiments is discussed in section 5. The results are summarized in section 6.

2. The need for ocean heat uptake efficacy

The GFDL CM2.1 and MPI ECHAM5 AOGCMs both report equilibrium sensitivity to CO_2 doubling of 3.4 ^{o}C. However, in transient experiments the MPI model appears to be

considerably more sensitive to forcing. The transient climate response (TCR), the temperature change at CO_2 doubling in a 1%/year CO_2 increase experiment, is nearly 50% greater for the MPI model (IPCC 2007, Table 8.2). The difference in transient sensitivity carries over to scenario forced experiments where the two models bracket the global temperature responses of most of the other models (IPCC, Fig. 10.5). Of 19 models listing transient climate responses in IPCC (2007) only four fall outside the range bounded by these two models. How might the zero-dimensional energy balance model account for the difference in transient response? This model represents the time-varying global-mean net TOA radiative flux N, as the sum of a forcing R and a term proportional to the global mean surface temperature anomaly, T:

$$N(t) = R(t) - \lambda T(t) \qquad (1)$$

Here N is positive down and λ is the climate feedback parameter. The MPI and GFDL models have similar equilibrium sensitivity, R/λ, and similar radiative forcing, R, so according to (1) the larger temperature response in the MPI model should be accounted for by a smaller net heat uptake, N.

Fig. 1 shows the global warming and net TOA flux anomalies for the two models forced with 1%/year CO_2 increase to doubling. Counter to (1), the MPI model has more heat uptake than the GFDL model. The heat uptake difference between the two models is evidently responding to the temperature change difference between the two models rather than forcing it, since the warmer model has more heat uptake. The 21st century

simulations of the two models under SRES B1, A1B and A2 forcing scenarios show similar relationships (not shown). Raper et al (2002) noted this tendency for models with larger transient warming to simulate larger heat uptake, relating the two quantities linearly with a constant of proportionality which they term "ocean heat uptake efficiency".

In this paper we take the view that the difference in transient response between these two models arises because the models respond differently to a given quantity of heat uptake. We do not propose a model for the ocean heat uptake itself as in Raper et al (2002) but are concerned instead with its impact on climate change which, as the above example shows, varies between models. To evaluate this impact we break the transient temperature change into the sum of an equilibrium temperature change, T_{EQ}, and disequilibrium temperature difference, T_{EQ}-T, driven by ocean heat uptake but with a feedback parameter that is smaller than that for CO_2 forcing by a factor of ε, the ocean heat uptake efficacy. We write the two equations for the different responses to radiative and heat uptake forcing as:

$$T_{EQ}(t) = R(t)/\lambda \qquad (2)$$

$$T_{EQ}(t)-T(t) = \varepsilon N(t)/\lambda \qquad (3)$$

One can think of these two equations as respectively representing the responses of a atmosphere/slab-ocean model, on time scales long compared to the equilibrium time scale of the slab, to the CO_2 perturbation and to the heat uptake. Subtracting (3) from (2) gives

$$T(t) = (R(t)-\varepsilon N(t))/ \lambda \qquad (4)$$

While R and λ are similar for the GFDL and MPI AOGCMs, ε is larger for the GFDL model causing it to have a smaller transient response, T. A large efficacy magnifies the effect of the heat uptake in the GFDL model and so its response lags that of the MPI model in time (Fig. 1).

Eqn. 4 is a generalization of (2), which is its ε=1 special case. By applying a factor to the ocean heat uptake in (4) we have not sacrificed conservation of energy. As (3) shows, ε modifies the feedback operating on ocean heat uptake. It is simply a matter convenience to attach it as a factor to N.

Hansen et al (1997) show that the geographical structure of a radiative forcing is an important source of non-unitary efficacy. They show that forcings focused at the surface at high latitudes have the greatest impact on temperature and therefore the larger efficacy. The ocean heat uptake occurs at the surface, of course, and it is largest in the subpolar oceans. Fig. 2 compares the doubled CO_2 radiative forcing with the ocean heat uptake at doubling in the 1%/year CO_2 increase experiment with the GFDL model. It is clear that the ocean heat uptake is enhanced at high latitudes while CO_2 forcing is somewhat larger

in the tropics. Therefore, the expectation is that ocean surface heat flux will tend to have an efficacy greater than 1.

While the first 70 years of the 1%/year CO_2 increase to doubling experiment contains responses to changes in both radiative forcing and heat uptake, the subsequent stabilization period gives us an opportunity to look at the response to changing ocean heat uptake in isolation. This experiment has been run for 600 years with the GFDL model and its global mean warming over the 530 year stabilization period is about the same as in the initial CO_2 increasing period. The efficacy in the stabilization period is about 2 – the model is twice as sensitive to ocean heat uptake as it is to CO_2 forcing, implying that that the feedback parameter for ocean heat uptake, λ/ε, is one half that for CO_2 forcing, λ (eqn. 3). To determine the sources of this difference, we evaluate feedbacks for the transient run stabilization period and the atmosphere/slab-ocean doubled CO_2 experiment using the kernel method of Soden and Held (2006) and the GFDL model radiative kernel. The results are shown in Table 1. The total feedback is about -1 $W/m^2/K$ for CO_2 forcing and -0.5 $W/m^2/K$ for ocean heat uptake. The 0.5 $W/m^2/K$ difference comes from the increased positive cloud and albedo feedbacks and a decreased negative temperature feedbacks in response to ocean forcing. Several studies show that water vapor and temperature feedbacks are tightly coupled through the maintenance of constant relative humidity (Zhang et al 1994; Soden and Held, 2006). This motivates combining of the temperature and water vapor feedback in Table 1, to avoid cancellation of large terms of opposite sign. The sum of these two increases the ocean heat uptake efficacy somewhat more than does the albedo feedback difference but less than the cloud feedback

difference. Thus the reasons for ocean heat uptake efficacy are distributed among the individual feedbacks with cloud feedback making the largest contribution, about 50% of the total difference in feedback, after combining temperature and water vapor feedbacks.

Having compared CO_2 and ocean heat uptake forcings and feedbacks we turn now to their temperature responses. We can use the long stabilization period to estimate the contribution of ocean heat uptake to the SST changes at the time of CO_2 doubling. The first step is to estimate the equilibrium response by extrapolating SST from the time of doubling to equilibrium (N=0) using the change with N over the stabilization period as the slope:

$$SST(\infty) \approx SST(70) + \left[SST(590) - SST(70)\right]\frac{N(70)}{N(70) - N(590)} \qquad (5)$$

where all fields represent twenty year averages centered at the given times and differences from the preindustrial control climate values. The estimated SST equilibrium response is shown in the top panel of Fig. 3. It is in general agreement with the equilibrium response of the atmosphere/slab-ocean model to CO_2 doubling (not shown) although the coupled model pattern has more fine structure due to changes in currents.

Having obtained the equilibrium SST response in this way we can use it to obtain the response forced by ocean heat uptake. Consistent with eqn. 3, this is simply the transient response (Fig 3, bottom panel) minus the equilibrium response and is shown in the middle panel of Fig. 3. Both ocean and CO_2 forcing induce SST responses that are

amplified in the subpolar regions. However the ocean forcing induces a stronger subpolar response so that the total response has a minimum of warming in these regions where the ocean forcing is dominant. This pattern is a common feature of transient simulations and appears in the IPCC (2007) multi-model mean. The pattern was noted by Manabe et al (1991) who showed that the deep mixed layers and large isopycnal mixing in the southern ocean and in the North Atlantic lead to minima in the ratio of transient to equilibrium response in those regions.

3. Ocean heat uptake efficacy with variable forcing and sensitivity

The difference in efficacy of the two models discussed in the last section was apparent because the models had similar equilibrium climate sensitivities and similar radiative forcings. We would also like to compare models with different sensitivities and also evaluate the efficacy in a single model, over time. For this purpose, we define the climate state, as illustrated schematically in Fig. 4, as consisting of the transient temperature change, T, relative to the equilibrium value, T_{EQ}, on the x-axis, and the net heat uptake, N, relative to the radiative forcing, R, on the y-axis.

The transient response to doubling, T(2X), is conventionally evaluated as a 20 year average centered on year 70 in a 1%/year increase of CO_2 experiment. At this time there will be a significant net flux, N(2X). It will prove useful to also consider the hypothetical equilibrium response $T_{EQ}(t)$ that would result if the climate system adjusted instantly to

the time-varying forcing. Since the equilibrium response to CO_2 is approximately linear in its forcing magnitude (Hansen et al 2005), a reasonable approximation is:

$$T_{EQ}(t) = T_{EQ}(2X)R(t)/R(2X) \quad (6)$$

The equilibrium response $T_{EQ}(2X)$ is assumed to be evaluated by integrating or extrapolating until N=0 (or using a slab ocean model to approximate this value), so that (6) and (2) imply

$$\lambda = R(2X)/T_{EQ}(2X) \quad (7)$$

Employing R(t) and $T_{EQ}(t)$ as scales we can use (6) and (7) to rewrite (4) as:

$$\varepsilon N(t)/R(t) = 1-T(t)/T_{EQ}(t) \quad (8)$$

This relationship is depicted on Fig. 4 by the shaded lines. The case $\varepsilon=1$ is shown as the straight line between [0, R] and [T_{EQ}, 0]. Climate states above this line have $\varepsilon<1$ and those below have $\varepsilon>1$. Lines of constant efficacy intersect at [T_{EQ}, 0]. The quantities T/T_{EQ} and N/R in (8) will be used in the following two sections to compare climate states in a single model as forcing varies over time (section 4) and compare models with different radiative forcings and climate sensitivities at the same point in time (section 5).

The effective climate sensitivity (Murphy, 1995) is the extrapolation of the transient climate state from [0, R] through [T, N] to N=0 (Fig. 4):

$$T_{EF}(t) = T(t)/(1-N(t)/R(t)) \quad (9)$$

A difference between $T_{EF}(2X)$ and $T_{EQ}(2X)$ implies a change in T_{EF} over time in order for $T_{EF}(t) \rightarrow T_{EQ}(2X)$ as $N \rightarrow 0$. Effective sensitivity will always vary in time unless the system stays on the line between [0, R] and [T_{EQ}, 0].

The effective forcing, R_{EF} (Williams, 2008) is obtained by extrapolating the climate state back to T = 0 using the CO_2 stabilized section of an AOGCM experiment. From (8), we can write this in terms of the efficacy as:

$$R_{EF} = R(2X) / \varepsilon \quad (10)$$

Thus effective forcing and efficacy of ocean heat uptake are closely related quantities, and both can be used to describe the time-variation of the effective sensitivity. Our preference is for the concept of efficacy because it clearly ties this differential response to the nature of the forcing. In our view the "tropospheric response" described by Williams et al is primarily an intrinsically coupled ocean-atmosphere transient phenomenon associated with the geographic pattern of ocean heat uptake rather than an atmosphere-only response analogous to the stratospheric adjustment to increased CO_2. Fast tropospheric responses analogous to stratospheric adjustment are possible, and can be

isolated in the switch-on mixed-layer simulations of Gregory and Webb (2008), or in fixed SST experiments with imposed forcings. This fast response is small in CM2.1 and is not related to the efficacy as defined here.

4. Time-evolution of efficacy in the GFDL CM2.1

We now focus on the time variation of the climate state in a single model, the GFDL CM2.1. This model has the largest efficacy at CO_2 doubling of any model in the IPCC ensemble presented in the next section. We employ the time-varying radiative forcing and equilibrium temperature change as scalings for the net TOA flux and transient temperature change, respectively, as in (8), to show the evolution of climate state over two 600 year experiments with a 1%/year CO_2 increase to doubling and to quadrupling. The results are shown in Fig. 5. The two experiments pass through a similar arc of states that have increasing efficacy over time, more rapidly at first, and then more gradually. There is a somewhat narrower band of efficacies in this arc in the 1% to four times CO_2 experiment -- presumably due to the larger signal to noise ratio. The scatter is larger in the transient forcing period of the experiments for the same reason. The two experiments are in reasonable agreement in this normalized climate state space, even in the band of states where the 1% to doubling experiment has stabilized forcing but the 1% to quadrupling experiment forcing is still increasing. The efficacy does not appear to be very sensitive to forcing history. The convergence of the model state on the lower right corner of Fig. 5 is an indication of the agreement of the coupled and slab-ocean

equilibrium sensitivities since the slab-ocean value has been used to normalize the temperature axis.

The descent from the $\varepsilon=1$ line in the 1%/year CO_2 increase experiments is seen to occur in the early pentads, while the forcing is ramping up. It should be noted that forcing increases alone do not induce efficacy – non-unitary efficacy develops as a climate response to forcing changes. To explore this early adjustment further, we also show the ensemble mean of four instantaneous CO_2 doubling experiments with the same model. The first four pentads of this ensemble mean are denoted on figure 5 with the "1" through "4" symbols. These show that the efficacy approaches a value near two within the first two decades. During this period a pattern is established of sea surface temperature change with reduced warming, and even some areas of cooling, in the subpolar North Atlantic and Southern oceans as the competing cooling effect of ocean heat uptake overcomes the radiatively forced response in these areas. The ocean warming that occurs in this early adjustment period is confined to the mixed layer and nearby regions.

Figure 5 also shows the mean state of a 5-member ensemble of 20^{th} century runs of CM2.1 averaged over the period 1980 to 1999 relative to an 1860 control run. The forcing is calculated as the change in top-of-atmosphere flux between two ensembles of fixed SST experiments, one with time-varying forcing agents and one with tine-invariant forcing agents. The late twentieth century climate state indicates that this model's high efficacy is applicable to the historical period as well as to idealized forcing experiments. An important implication is that accurate measurements of the temperature change,

forcing and ocean heat uptake associated with anthropogenic forcing in the current climate will not be sufficient to determine the equilibrium climate sensitivity and the committed warming if the actual heat uptake efficacy is significantly different from unity, as it is in this model.

The 600 year time series of pentadal and global mean temperature changes for the CM2.1 1%/yr to doubling experiment is shown in Fig 6. This time series shows that about half of the total warming occurs in the CO_2-stabilized portion of the run. If we use eqn. 8 for the fit, taking the heat uptake from the model itself, with an efficacy of 1, there is too much warming in the CO_2 increasing period and not enough in the CO_2 stabilized period although this fit seems to be approaching the AOGCM's temperature at the end of the experiment. If we use an effective sensitivity in place of the equilibrium sensitivity in the equation, as is commonly done in reduced model fits to AOGCMs, a similar but smaller bias is apparent early in the run. Although this fit works reasonably well in the first two centuries, it has insufficient temperature increase in the final 400 years of the experiment.

The use of an efficacy allows us to fit both the CO_2 increasing and CO_2 stabilized portions of the time series. However, applying the efficacy naively to all timescales has the effect of increasing the amplitude of short term temperature variations. This suggests that these short term variations in N are not subject to the same efficacy as the longer term variations, as would be plausible if these are not as concentrated in high latitudes as the long term evolution of N –ENSO variability for example. An efficacy parameter

should be useful in the simple models that are fit to AOGCMs when it is desirable to capture the long-term behavior of the AOGCM.

5. Multi-model transient efficacies at CO_2 doubling

We turn now from the time evolution of efficacy in a single model to the inter-model variation of efficacy and related parameters in the IPCC AOGCMs, evaluated at CO_2 doubling in 1%/year CO_2 increase experiments. The IPCC reports contain doubled CO_2 forcing, transient climate response, equilibrium sensitivity, and effective sensitivity for a large number of AOGCMs. For a group of 14 models used for the IPCC Fourth Assessment Report (2007) with doubled CO_2 forcing, R(2X), available in the report, we used the published equilibrium climate sensitivity values in conjunction with T(2X) and N(2X) calculated from CMIP3 data. For a group of 8 IPCC Third Assessment Report (2001) models we used the published values of T(2X), $T_{EQ}(2X)$ and $T_{EF}(2X)$ to calculate N(2X)/R(2X) using:

$$N(t)/R(t) = 1-T(t)/T_{EF}(t), \quad (11)$$

obtained by rearranging (9), and ε(2X) using:

$$\varepsilon(t) = (1-T(t)/T_{EQ}(t))/(1-T(t)/T_{EF}(t)) \quad (12)$$

obtained by combining (8) and (9). To calculate N from N/R we use the doubled CO_2 radiative forcing listed in IPCC (2001) when available and the mean of the other models, when not. The models used and their parameter values are listed in Table 2. There are some small differences between the transient climate responses in Table 2 and those given in the report for the AR4 models owing to differences in the treatment of the control. Here we have used averages over the 140 year period of the control run centered on the time of doubling in the perturbation run. The parameters in the table correspond to terms in

$$T = T_{EQ}(1-\varepsilon N/R) \qquad (13)$$

which is eqn. 8 rearranged. The inter-model correlations of these parameters are shown in Table 3. Figure 7 shows climate model transient climate responses (normalized by their equilibrium sensitivities) and net top-of-atmosphere fluxes (normalized by their radiative forcings) at CO_2 doubling. Figure 7 and Table 2 show that the great majority the models have an efficacy greater than one. The mean efficacy is 1.34. The two generations of models have similar distributions of efficacies.

Table 3 shows that the radiative forcing has little correlation with transient and equilibrium warming. The methodology for computing radiative forcings in not fully standardized, and it is likely that the inter-model spread of forcing values would be smaller with more standardization, so it is encouraging that the mean and standard deviation of efficacy in the models is not altered substantially if one substitutes a uniform

value of the forcing for the tabulated values. Some of the lowest values of efficacy are eliminated if one uses a uniform forcing, however.

T_{EQ} , ε and N are well correlated with T, the transient climate response (TCR) and the sign of the correlations is such that T_{EQ} and ε variations enhance the inter-model TCR differences while N variations damp them. T_{EQ} is the most difficult to diagnose. Since (13) defines ε, it would be possible for ε to capture spurious variance from misdiagnosis of T_{EQ}. The lack of correlation between the two parameters allays this concern. We conclude that efficacy is an important driver of inter-model TCR variance in addition to, and relatively independent of, the equilibrium sensitivity.

The right side of (13), $1-\varepsilon N/R$, is anti-correlated with T_{EQ} (ρ=-0.56) but poorly correlated with TCR (ρ=0.20). It is of interest that ε can have a stronger association with TCR than T_{EQ} in spite of its confinement within a term which has a poor correlation with TCR. The key is correlation of N with the other parameters. Following Gregory and Mitchell (1997) and Raper et al (2002) and noting the inter-model correlation of N and TCR, we make use of the ocean heat uptake efficiency, γ , defined by

$$N = \gamma T \qquad (14)$$

Note that efficiency represents ocean mixing processes while efficacy represents radiative processes in response to ocean heat flux. The heat uptake parameterization (14) essentially treats the ocean as an infinite reservoir – it does not account for impact of

ocean warming on reducing N that is evident in the stabilized CO_2 section of the experiments (Fig. 1), for example. Nevertheless, it is useful for comparing models when forcing is rapidly increasing and a dynamic balance is established between radiative forcing of temperature anomalies and the sum of their damping to space and to the deep ocean. Using (14) in (13), along with $\lambda=R/T_{EQ}$, we obtain an alternative expression for the degree of equilibration:

$$T/T_{EQ} = 1-\varepsilon N/R = 1/(1+\varepsilon\gamma/\lambda) \qquad (15)$$

This expression is a generalization for efficacy of a similar relationship derived in Raper et al (2002). As was noted by Raper et al and others, more sensitive models, with smaller λ, have less equilibrated surface temperature responses. The appearance of λ ($=R/T_{EQ}$) in (15) is a source of anti-correlation between T_{EQ} and $1-\varepsilon N/R$.

While λ effects TCR through T_{EQ} as well as through the degree of equilibiration, ε and γ have their impact on the TCR entirely through the degree of equilibration. Table 4 shows the correlation of these three parameters with T/T_{EQ}. The signs of the correlations are consistent with (15). Efficacy has the largest correlation with TCR/T_{EQ} but little correlation with the efficiency, γ. The correlation of ε with N (Table 3) is apparently accounted for by its correlation with TCR after assuming (14). In this view the anti-correlation between ε and N comes about because efficacy reduces warming by enhancing the cooling effect of heat uptake; the reduced warming, in turn, feeds back to reduce heat uptake.

Equation 15 expresses the simple idea that equilibration is decreased by a large ratio of γ, deep-ocean/surface climate coupling, to λ/ε, the coupling of the resultant anomalies to space. The degree of equilibration in the multi-model global mean is a little greater than ½, indicating that this ratio is near 1, the strength of coupling to space and to the deep ocean are about the same. Mathematically, efficacy and efficiency enter as a product in (15) and Figure 8 shows the impact of their inter-model variation on the product. The variations in efficacy are responsible for most of the variation in the product, so that, as expected from the correlations in Table 4, it has a larger influence on the degree of equilibration.

The implication of our simple model interpretation is that one would be more effective in reducing AOGCM uncertainties in transient climate sensitivity by reducing uncertainty in the radiative response to ocean heat uptake than in the relationship of the uptake magnitude to the surface climate perturbation. Uncertainty in radiative feedbacks substantially impacts not only the simulated equilibrium response but also the trajectory toward equilibrium for which ocean processes might have been thought dominant.

6. Conclusions

We argue that simple energy balance model fits to AOGCMs should make use of the concept of the efficacy of ocean heat uptake. This is equivalent to, but we believe more physically intuitive than, the concept of "effective forcing" since the adjustments that establish efficacy or effective forcing take place on a decadal scale, favoring

interpretation as a response rather than a forcing. We also show that efficacy is more parsimonious than "effective sensitivity" since a considerable part of the time-dependence of effective sensitivity can be captured with a time-invariant efficacy. The efficacy factor is variable across the AOGCMs used for IPCC assessments but is generally larger than 1 with an average value between 1.3 and 1.4, and can approach 2. Thus for most models the simulated warming is more sensitive to ocean heat uptake than to CO_2 radiative forcing. Amongst the models, the transient climate response is better correlated with the efficacy than it is with the equilibrium climate sensitivity. The efficacy and climate sensitivity have little correlation, indicating that they represent different model characteristics. An understanding of the reasons for the differences in efficacy amongst the models should be useful for resolving the differences in the magnitude of transient climate change simulated in these models.

The use of an efficacy, or its equivalent, is necessary to fit the global mean temperature in both the forcing-increasing and forcing-stabilized sections of a 1%/year CO_2 increase experiment with the GFDL CM2.1. The potential significance of high efficacy in slowing the warming is well illustrated by this model and by an analysis of models utilized in the third and fourth IPCC assessments. The stabilized forcing warming commitment inherent in a given level of ocean heat uptake is magnified by the efficacy. High efficacy implies a greater fraction of the equilibrium response will occur after stabilization. Therefore uncertainty about efficacy poses a difficulty for determination of the equilibrium climate sensitivity from observations of forcing, temperature, and ocean heat uptake.

Plattner et al (2008) and Solomon et al (2009) have presented the long term response to CO_2 emissions in intermediate complexity models. In these experiments, there is a near cancellation between the warming effect of reduced ocean heat uptake and the cooling effect of reduced radiative forcing as carbon enters the ocean in the millennium following a cessation of carbon emissions, leading to a global temperature that declines only slightly. Our study indicates that radiative feedbacks play an important role in the impact of the ocean heat uptake reductions and that different AOGCMs may give differing results due to differences in the efficacy of heat uptake. A larger heat uptake efficacy would imply a more durable temperature response to CO_2 emissions as reduction in radiative forcing accompanying oceanic CO_2 uptake experiences a relatively larger warming offset from reduced ocean heat uptake. Our results suggest that the AOGCMs, which contain the most comprehensive simulations of radiative feedbacks and efficacy, should be applied to this long term emissions commitment problem.

Acknowledgments

The authors thank Ron Stouffer, Geoff Vallis, Rong Zhang and four anonymous reviewers for helpful comments on the manuscript. The authors also thank Brian Soden for the use of the GFDL CM2.1 radiative kernel. The authors acknowledge the international modeling groups for providing their data for analysis, the Program for Climate Model Diagnosis and Intercomparison (PCMDI) for collecting and archiving the model data, the JSC/CLIVAR Working Group on Coupled Modeling (WGCM) and their

Coupled Model Intercomparison Project (CMIP) and Climate Simulation Panel for organizing the model data analysis activity, and the IPCC WG1 TSU for technical support. The IPCC Data Archive at Lawrence Livermore National Laboratory is supported by the Office of Science, U.S. Department of Energy.

References

Boer, G.J., and B. Yu, 2003: Dynamical aspects of climate sensitivity, *Geophys. Res. Lett*., **30**(3), doi:10.1029/2002GL016549.

Gregory, J.M., and J.F.B. Mitchell, 1997: The climate response to CO2 of the Hadley Centre coupled AOGCM with and without flux adjustments, *Geophys. Res. Lett.*, **24**, 1943-1946.

Gregory, J.M., et al, 2004: A new method for diagnosing radiative forcing and climate sensitivity, *Geophys. Res. Lett*., **31**, L03205, doi:10.1029/2003GL018747.

Gregory and Webb, 2008: Tropospheric adjustment induces a cloud component in CO2 forcing. J. Climate 21 (1) 58-71

Hansen, J., M. Sato, and R. Ruedy, 1997 : Radiative forcing and climate response, *J. Geophys. Res.*, **102**(D6), 6831—6864.

Hansen, J. et al, 2005: Efficacy of climate forcings. *J. Geophys. Res*., **110**, D18104, doi:10.1029/2005JD005776.

IPCC 2001: Climate Change 2001: The Scientific Basis. Contribution of Working Group I to the Third Assessment Report of the Intergovernmental Panel on Climate Change. Cambridge University Press, 881 pp.

IPCC 2007: Climate Change 2007: The Scientific Basis. Contribution of Working Group I to the Fourth Assessment Report of the Intergovernmental Panel on Climate Change. Cambridge University Press, 996 pp.

Manabe, S., R.J. Stouffer, M.J. Spelman, and K. Bryan, 1991: Transient response of a coupled ocean atmosphere model to gradual changes of atmospheric CO2. Part I: Annual mean response, *J. Climate*, **4**, 785—818.

Meinshausen, M., S.C.B. Raper, and T.M.L. Wigley, 2008: Emulating IPCC AR4 atmosphere-ocean and carbon cycle models for projecting global-mean, hemispheric and land/ocean temperatures: MAGICC 6.0, Atmos. *Chem. Phys. Discuss.*, **8**, 6153—6272.

Murphy, J.M., 1995: Transient response of the Hadley Centre coupled ocean-atmosphere mode to increasing carbon dioxide. Part III: Analysis of global-mean response using simple models*, J. Clim*., **8**, 496-514.

Plattner, G.-K, R. Knutti, F. Joos, T.F. Stocker, W. von Bloh, V. Brovkin, D. Cameron, E. Driesschaert, S. Dutkiewicz, E. Eby, N Edwards, T. Fichefet, J. Hargreaves, C. Jones, M. Loutre, H. Matthews, A. Mouchet, S. Müller, S. Nawrath A. Price, A. Sokolov, 2008:

Long-term climate commitments projected with climate-carbon cycle models, *J. Climate*, **21**, 2721-2751.

Raper, S.C.B., J.M. Gregory, and R.J. Stouffer, 2002: The role of climate sensitivity and ocean heat uptake on AOGCM transient temperature response, *J. Clim*., **15**, 124-130.

Senior, C. A., and J.F.B. Mitchell, 2000: Time-dependence of climate sensitivity, *Geophys. Res. Lett*., **27**(17), 2685-2688.

Soden, B.J., and I.M. Held, 2006: An assessment of climate feedbacks in coupled ocean-atmosphere models, *J. Climate*, **19**, 3354—3360.

Solomon, S., G-K Plattner, R. Knutti, and P. Friedlingstein, 2009: Irreversible climate change due to carbon dioxide emissions, *Proc. Nat. Academy of Sciences*, **106**, 1704—1709.

Watterson, I.G., 2000: Interpretation of simulated global warming using a simple model, *J. Climate*, **13**, 202-215.

Williams, K.D., W.J. Ingram, and J.M. Gregory, 2008: Time variation of effective climate sensitivity in GCMs, *J. Climate*, 21, 5076—5090.

Zhang, M. H., J. J. Hack, J. T. Kiehl, and R. D. Cess (1994), Diagnostic study of climate feedback processes in atmospheric general circulation models, *J. Geophys. Res.*, 99(D3), 5525–5537.

List of Tables

List of Figures

Fig. 4. Schematic relationships between radiative forcing R, equilibrium climate sensitivity T_{EQ}, effective climate sensitivity T_{EF}, effective forcing R_{EF}, and ocean flux efficacy ε, on a plot of global mean temperature T, against net top-of-atmosphere heat flux N. N is nearly equal to the net ocean heat flux over climatological timescales. If the climate state traverses the thick gray line between [0, R] and [T_{EQ}, 0], R_{EF}=R, ε =1, and T_{EF}=T_{EQ}. T_{EF}, R_{EF} and ε are different ways of accounting for deviations of the climate state from this path.

Fig. 5. A scatter plot of scaled global mean temperature T/T_{EQ} against scaled top-of-atmosphere net heat flux N/R for the 1% CO_2 increase to doubling and quadrupling experiments with the GFDL CM2.1 climate model. All points are pentadal averages. The first three pentads of the 1%/year experiments fall outside the box due to smallness of the forced response early in the experiments. The numbers represent pentadal and 4-member ensemble means from the first 20 years of an instantaneous CO_2 doubling experiment with the same model. The green circle shows the mean state of 5-member ensemble of 20th century runs between 1980 and 1999.

Fig. 6. Time series of pentadally averaged global mean temperature change in the 1% per year CO_2 increase to doubling experiment of the GFDL CM2.1 climate model. The plot also shows estimates of the transient temperature change using eqn. 8 with an efficacy of 2 and eqn. 10 with an effective climate sensitivity of 2.28^{o}C.

Fig. 7. Scatter plot of global mean temperature at CO_2 doubling scaled by the equilibrium temperature change (T/T_{EQ}) against net top-of-atmosphere heat flux scaled by the doubled CO_2 radiative forcing (N/R) for 22 climate models used in the IPCC third and fourth assessment reports. Twenty year means centered on year 70 of the 1% CO_2 increase per year to doubling experiments are used for the estimates.

Fig. 8. Scatter plot of the ocean heat flux efficacy against efficiency for 22 climate models used in the IPCC third and fourth assessment reports. The product of the two scattered quantities reduces the equilibration of the surface climate, TCR/T_{EQ}.

Table 1. GFDL CM2.1 radiative feedbacks ($W/m^2/K$).

	CO_2 Forced	**Ocean Heat Uptake Forced**	**CO_2 – OHU**
Temperature + Water Vapor	-2.14	-1.96	-0.18
Albedo	0.31	0.39	-0.08
Cloud	0.81	1.04	-0.23
Total	-1.03	-0.53	-0.50

Table 2. IPCC AOGCM global parameters (eqn. 13) at CO_2 doubling in 1%/year CO_2 increase experiment.

Model[a]	TCR K	T_{EQ} K	N W/m^2	R W/m^2	ε
CCCma CGCM1[b]	2.0	3.5	1.64	3.60	0.97
CSIRO MK2	2.0	4.3	1.59	3.45	1.16
NCAR CSM1	1.4	2.1	0.89	3.60	1.29
GFDL R15a[b]	2.1	3.7	1.76	3.60	0.86
UKMO HADCM2	1.7	4.1	1.11	3.47	1.83
MRI1[b]	1.6	4.8	1.30	3.60	1.85
MRI2[b]	1.1	2.0	0.96	3.60	1.69
DOE PCM	1.3	2.1	0.91	3.60	1.56
CCCMA CGCM3.1	1.9	3.4	1.17	3.32	1.25
CSIRO MK3.0	1.5	3.1	1.32	3.47	1.39
GISS MODEL EH	1.6	2.7	1.27	4.06	1.34
GISS MODEL ER[c]	1.5	2.7	1.50	4.06	1.19
GFDL CM2.0	1.5	2.9	0.92	3.50	1.85
GFDL CM2.1	1.5	3.4	1.00	3.50	1.99
IPSL CM4	2.1	4.4	1.57	3.48	1.18
MPI ECHAM5	2.1	3.4	1.31	4.01	1.16
MIROC 3.2 MEDRES	2.0	4.0	1.63	3.09	0.94
MIROC 3.2 HIRES	2.7	4.3	1.61	3.14	0.74
MRI CGCM2.3.2A	2.2	3.2	1.21	3.47	0.92
NCAR CCSM3.0	1.5	2.7	1.10	3.95	1.65
UKMO HADCM3[d]	2.1	3.8	1.23	3.81	1.42
UKMO HADGEM1[d]	1.9	3.4	1.34	3.78	1.25
Mean	1.8	3.4	1.29	3.60	1.34
St. Dev.	0.37	0.78	0.27	0.26	0.35
Coef. of Var.	0.21	0.23	0.21	0.07	0.26

Notes:

a) TAR model (italicized) TCRs and T_{EQ}s are taken from Table 9.1 of IPCC (2001); AR4 model T_{EQ}s are from Table 8.2 of IPCC (2007) except where noted. The CCSR NIES2 model was available in Table 9.2 of IPCC 2001 but has been excluded from this study because its effective sensitivity of 11.6 ^oC makes it an outlier in the combined ensemble. The global temperature and net TOA flux changes for the AR4 models were calculated from CMIP3 database data using the differences between 20 year averages taken at CO_2 doubling and a 140 year period, centered on the time of doubling, from the control runs. The doubled CO_2 forcings are taken from Table 10.2 of IPCC (2007).

b) R was not available. The mean R of the reporting models (3.6 Wm^{-2}) was used.

c) Year 70 in 1% CO_2 increase per year to 4x experiment was used.

d) T_{EQ}s estimated by extrapolation from long transient experiments taken from Table 2 of Williams et al (2008).

Table 3. IPCC AOGCM global parameter inter-model correlations (eqn. 13).

	TCR	T_{EQ}	N	R	ε
TCR	1	0.68	0.71	-0.33	-0.74
T_{EQ}		1	0.62	-0.41	-0.20
N			1	-0.16	-0.74
R				1	0.19
ε					1

Table 4. IPCC AOGCM global parameter inter-model correlations (eqn. 15).

	TCR/T_{EQ}	λ	ε	γ
TCR/T_{EQ}	1	0.50	-0.57	-0.32
λ		1	0.26	0.18
ε			1	-0.03
γ				1

Fig. 1. Global mean temperature anomaly (top) and net top-of-atmosphere radiation anomaly (bottom) for the GFDL CM2.1 and MPI ECHAM5 AOGCMs forced with the 1%/year CO_2 increase to doubling. Anomalies are taken relative to the mean of the first century of the pre-industrial control runs. The equilibrium temperature change and radiative forcing are taken from IPCC (2007).

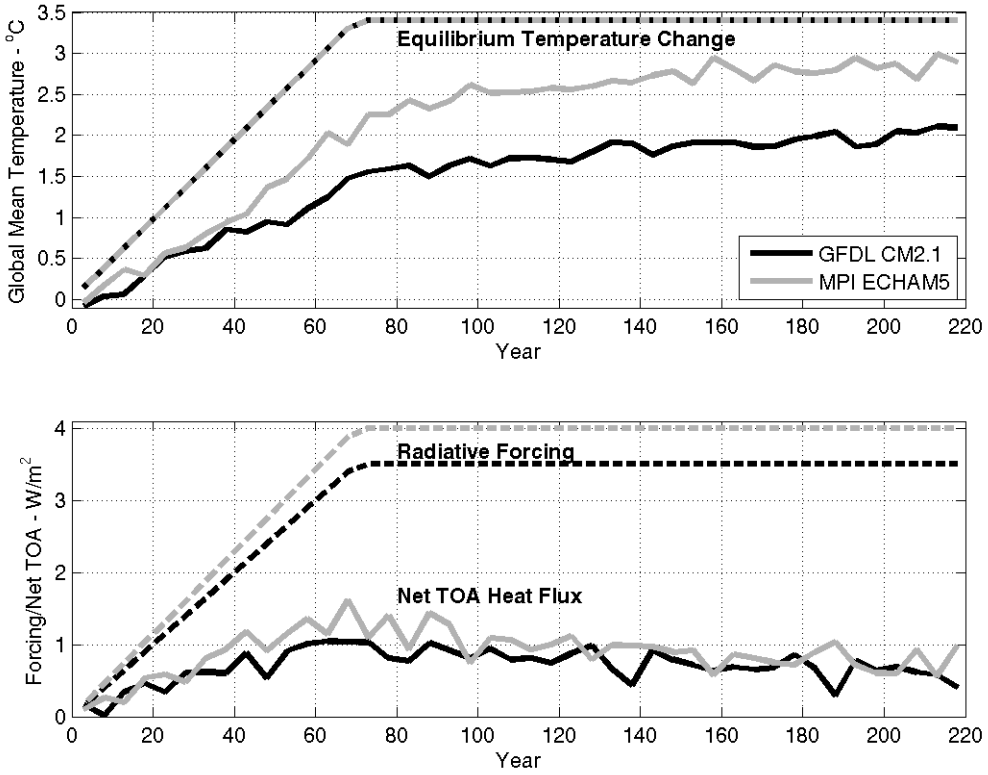

Fig. 2. Zonal mean doubled CO_2 radiative forcing and ocean heat uptake at doubling in the 1%/year CO_2 increase experiment of GFDL CM2.1.

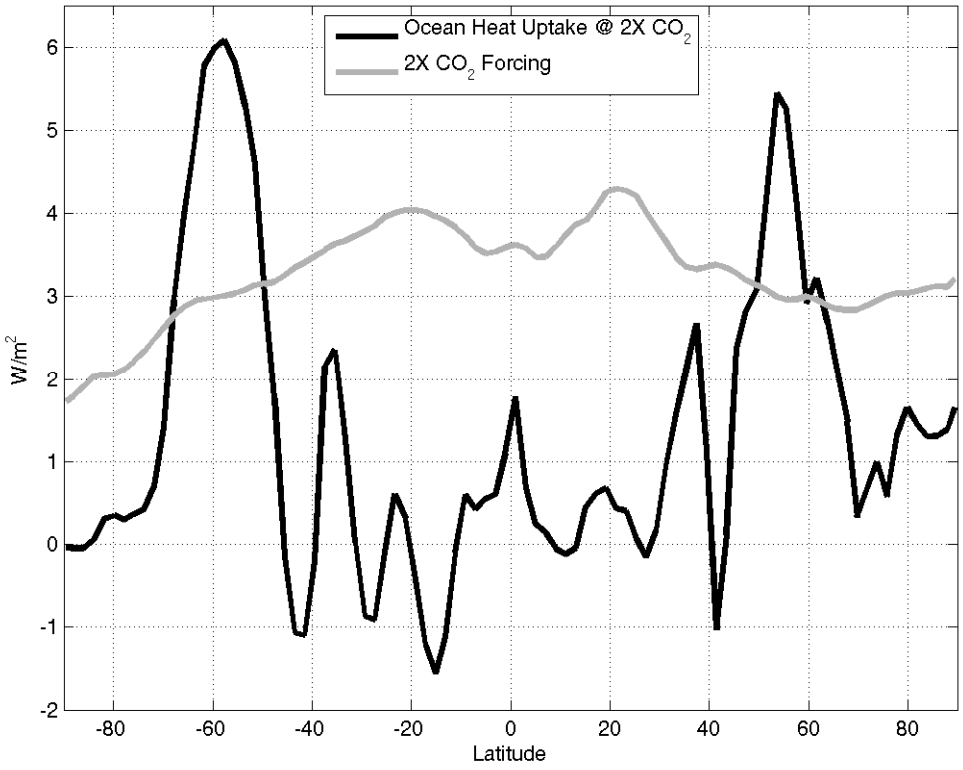

Fig. 3. SST equilibrium response (°C) to a CO_2 doubling estimated from a long coupled model run of a 1%/year CO_2 increase to doubling experiment using eqn. 5 (top), ocean heat uptake forced component of the transient response at CO_2 doubling (middle) and the transient response at CO_2 doubling (bottom). The bottom panel is sum of the top and middle panels.

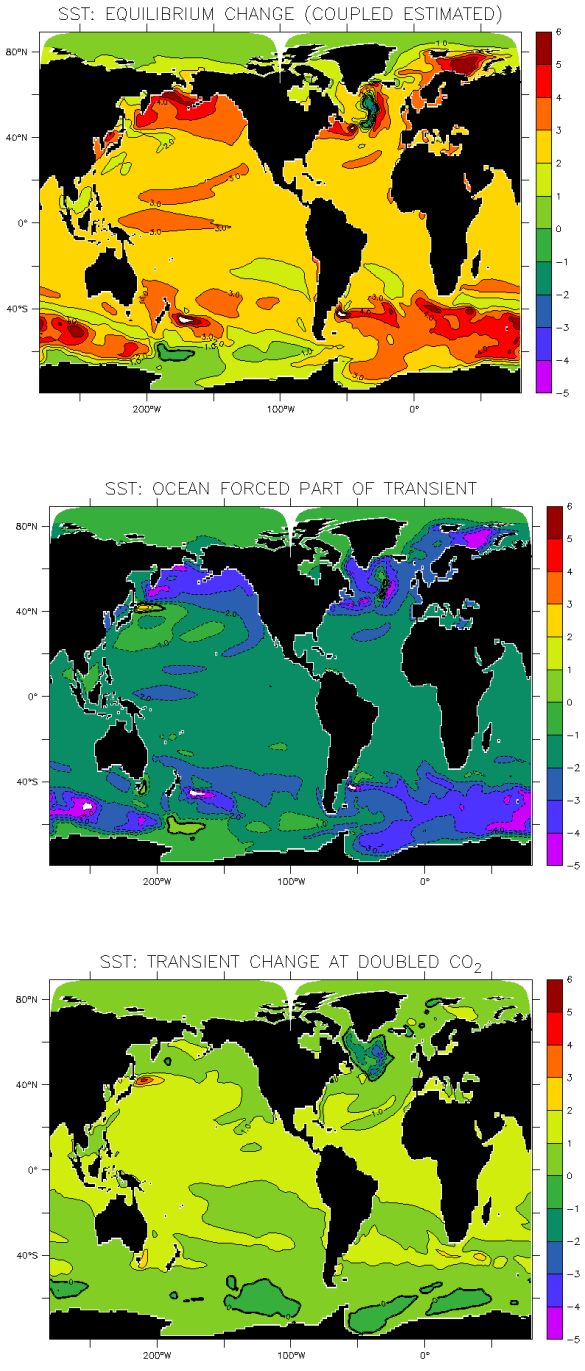

Fig. 4. Schematic relationships between radiative forcing R, equilibrium climate sensitivity T_{EQ}, effective climate sensitivity T_{EF}, effective forcing R_{EF}, and ocean flux efficacy ε, on a plot of global mean temperature T, against net top-of-atmosphere heat flux N. N is nearly equal to the net ocean heat flux over climatological timescales. If the climate state traverses the thick gray line between [0, R] and [T_{EQ}, 0], R_{EF}=R, ε =1, and T_{EF}=T_{EQ}. T_{EF}, R_{EF} and ε are different ways of accounting for deviations of the climate state from this path.

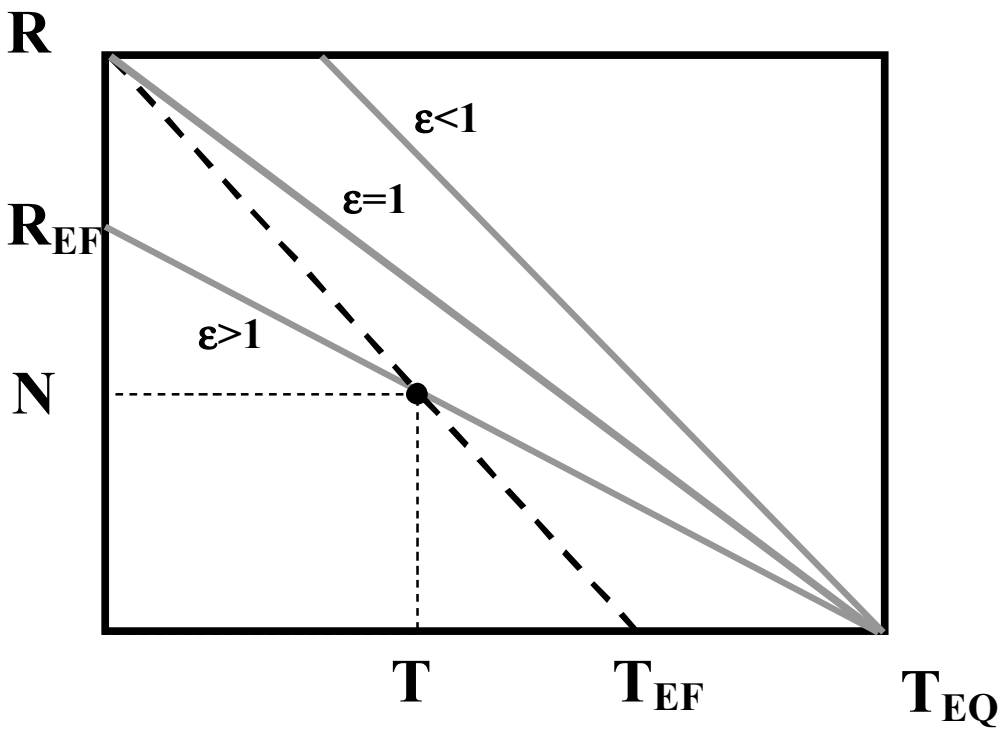

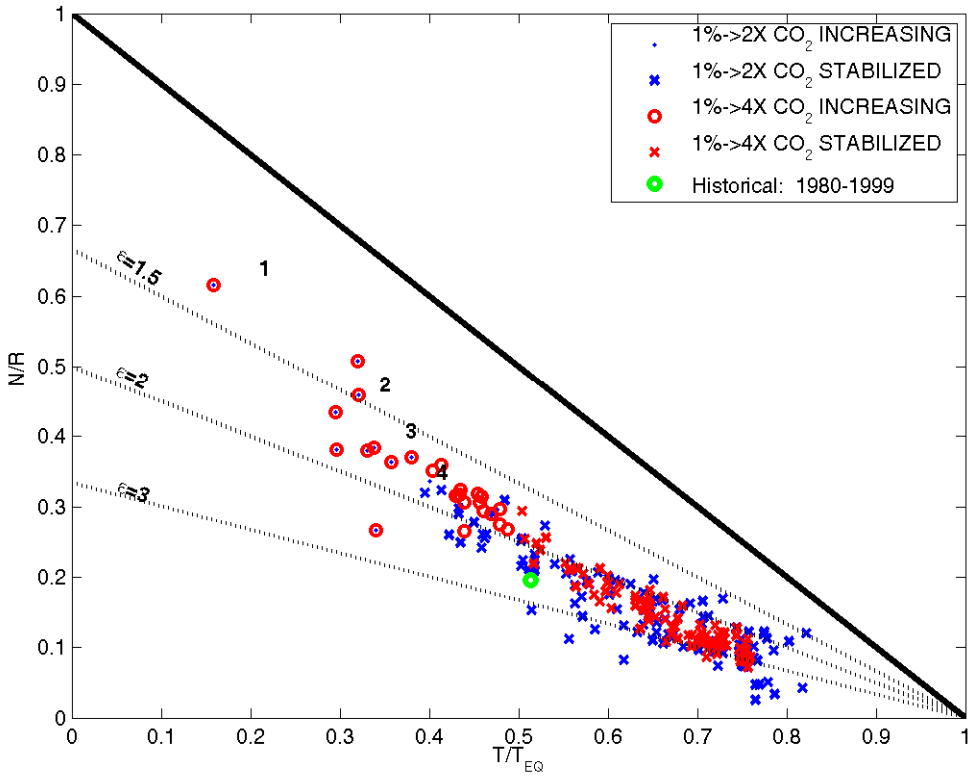

Fig. 5. A scatter plot of scaled global mean temperature T/T_{EQ} against scaled top-of-atmosphere net heat flux N/R for the 1% CO_2 increase to doubling and quadrupling experiments with the GFDL CM2.1 climate model. All points are pentadal averages. The first three pentads of the 1%/year experiments fall outside the box due to smallness of the forced response early in the experiments. The numbers represent pentadal and 4-member ensemble means from the first 20 years of an instantaneous CO_2 doubling experiment with the same model. The green circle shows the mean state of 5-member ensemble of 20th century runs between 1980 and 1999.

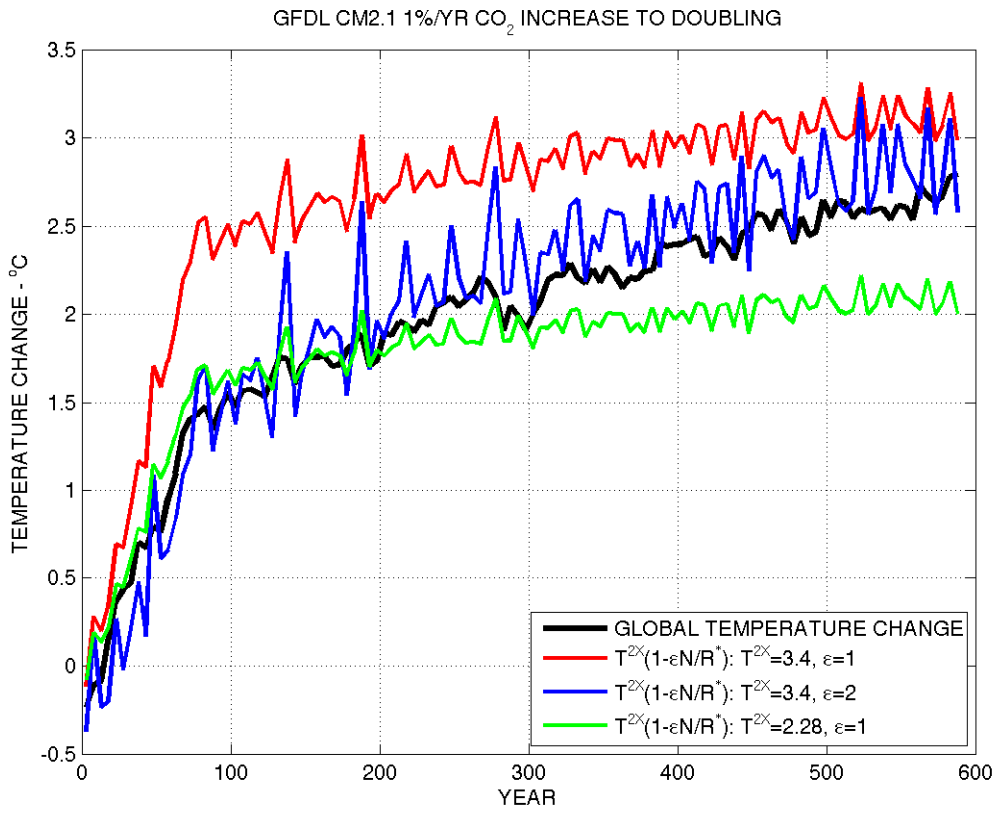

Fig. 6. Time series of pentadally averaged global mean temperature change in the 1% per year CO_2 increase to doubling experiment of the GFDL CM2.1 climate model. The plot also shows estimates of the transient temperature change using eqn. 8 with an efficacy of 2 and eqn. 10 with an effective climate sensitivity of 2.28°C. This value was used in IPCC 2007 to fit a simple climate model to mimic the GFDL CM2.1 (see Table S8.1).

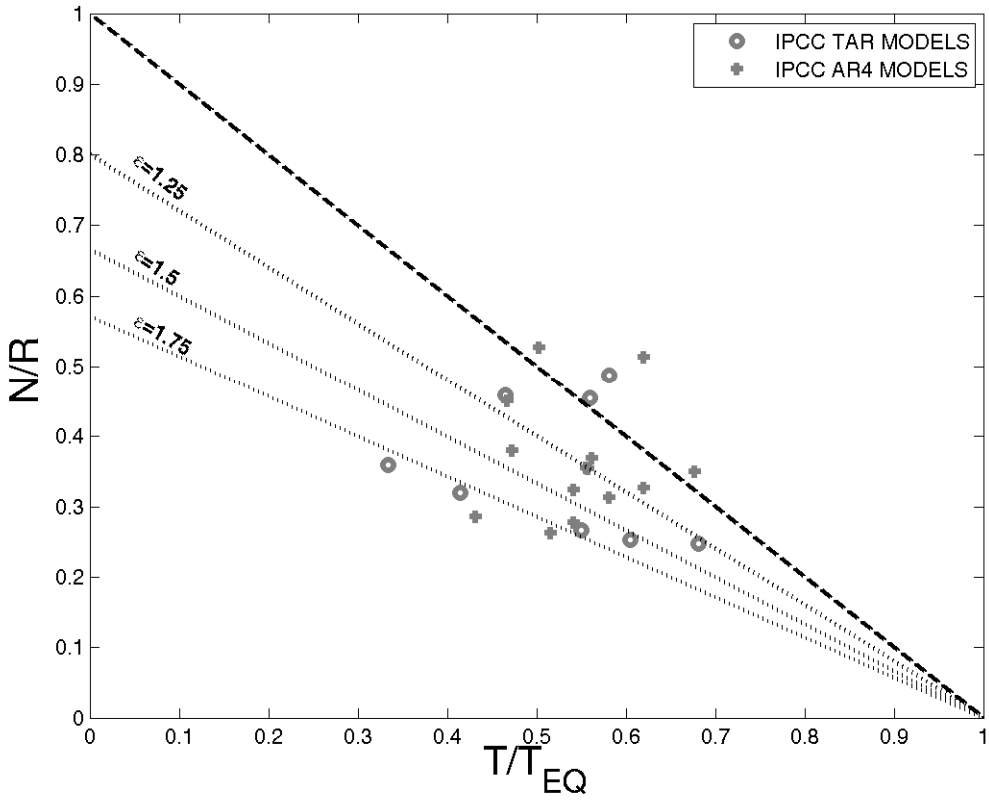

Fig. 7. Scatter plot of global mean temperature at CO_2 doubling scaled by the equilibrium temperature change (T/T_{EQ}) against net top-of-atmosphere heat flux scaled by the doubled CO_2 radiative forcing (N/R) for 22 climate models used in the IPCC third and fourth assessment reports. Twenty year means centered on year 70 of the 1% CO_2 increase per year to doubling experiments are used for the estimates.

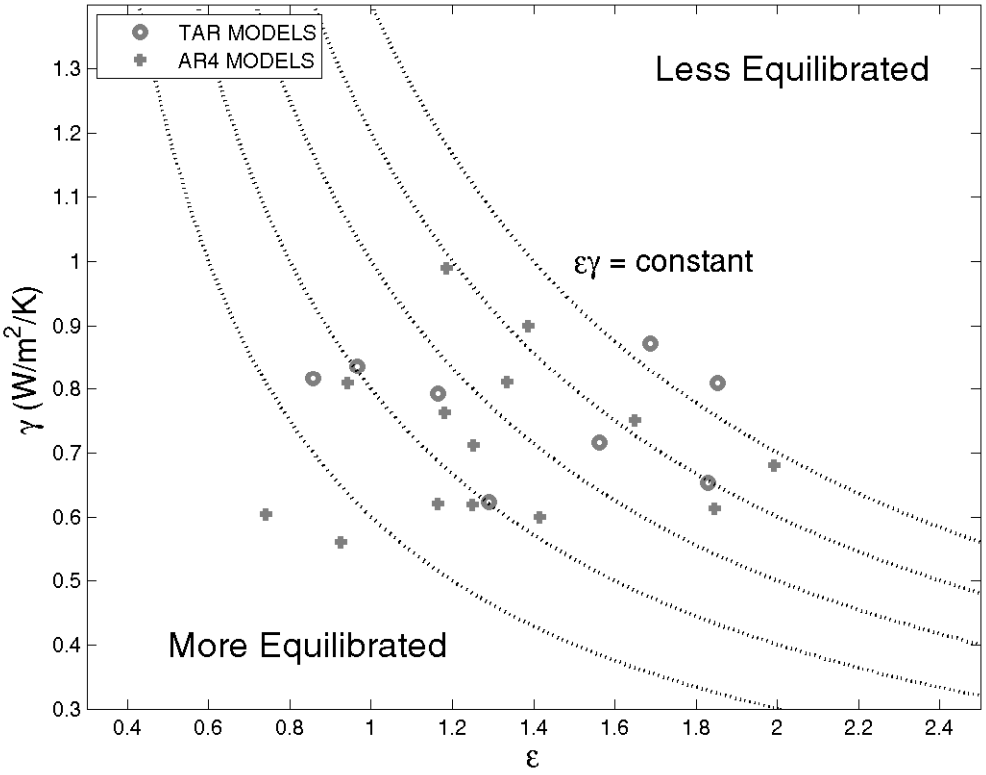

Fig. 8. Scatter plot of the ocean heat flux efficacy against efficiency for 22 climate models used in the IPCC third and fourth assessment reports. The product of the two scattered quantities reduces the equilibration of the surface climate, TCR/T_{EQ}.